

Optimization based inversion method for the inverse heat conduction problems

Huaiping Mu^{1,*}, Jingtao Li¹, Xueyao Wang² and Shi Liu¹

¹School of Energy, Power and Mechanical Engineering, North China Electric Power University, Beijing, China

²Institute of Engineering Thermophysics, Chinese Academy of Sciences, Beijing, China

*Corresponding author e-mail: muhuaipingdr@126.com

Abstract. Precise estimation of the thermal physical properties of materials, boundary conditions, heat flux distributions, heat sources and initial conditions is highly desired for real-world applications. The inverse heat conduction problem (IHCP) analysis method provides an alternative approach for acquiring such parameters. The effectiveness of the inversion algorithm plays an important role in practical applications of the IHCP method. Different from traditional inversion models, in this paper a new inversion model that simultaneously highlights the measurement errors and the inaccurate properties of the forward problem is proposed to improve the inversion accuracy and robustness. A generalized cost function is constructed to convert the original IHCP into an optimization problem. An iterative scheme that splits a complicated optimization problem into several simpler sub-problems and integrates the superiorities of the alternative optimization method and the Broyden-Fletcher-Goldfarb-Shanno (BFGS) algorithm is developed for solving the proposed cost function. Numerical experiment results validate the effectiveness of the proposed inversion method.

1. Introduction

The IHCP analysis method is often employed to estimate the thermal physical parameters of materials, boundary conditions, initial conditions, heat flux, heat sources, etc., from the given temperature measurement data in the field of the thermal engineering. In light of providing an effective way for acquiring such parameters, the IHCP method has attracted growing attentions.

The efficiency of the inversion algorithms has a great influence on applications of the IHCP method. A variety of algorithms have been developed for solving the IHCP, e.g., the Levenberg-Marquardt method [1, 2], the conjugate gradient technique [3, 4], the standard Tikhonov regularization (STR) algorithm [5], the particle swarm optimization technique [6, 7], etc. The interesting readers can refer to [8-15] for more details. In light of the complexity of the problem, generally, figuring out an inversion algorithm with low computational cost and high inversion accuracy remains a crucial issue.

The ill-posed nature of the IHCP will give rise to a formidable quandary, i.e., small perturbations on the input data may lead to larger fluctuations of the inversion solutions, which may make the final results meaningless. Conventional inversion algorithms emphasize the measurement errors and fail to



take into account the inaccurate properties on the forward problem derived from the facts such as (1) the assumptions and simplifications of a real physical problem; (2) the imprecise initial conditions, boundary conditions, geometric conditions and thermal physical properties of materials; and (3) the discretization of the original problem and the approximation of the numerical computation. As a result, developing an algorithm that simultaneously highlights the inaccurate properties of the measurement data and the forward problem may be essential for improving the inversion precision. In this work an inversion model is put forward to simultaneously underline the inaccurate properties of the forward problem and the measurement data is proposed to improve the inversion accuracy and robustness. A cost function is constructed to convert the original IHCP into an optimization problem. An efficient algorithm is developed for searching for the optimal solution of the proposed cost function. Numerical experiment results validate effectiveness of the proposed method.

2. Mathematical model

There are two key steps in seeking for the solution of the IHCP: the forward problem and the inverse problem. In this section, we first revisit the mathematical models for the IHCP.

2.1. Forward problem

By means of employing an effective numerical method, e.g., the finite element method, the finite volume method, etc., the forward problem estimates the temperature distribution from the given conditions of the determined solutions, which can be specified as follows [16]:

$$\rho c_p \frac{\partial T}{\partial t} = \nabla \cdot (\lambda \nabla T) \quad (1)$$

where ρ , c_p and λ mean the density, heat capacity and heat conductivity coefficient, respectively; T represents the temperature distribution and t implies the time index.

2.2. Traditional inversion model

The inverse problem estimates initial conditions, boundary conditions or thermal physical parameters of materials from the given temperature measurement data. For compact notation, the inverse problem can be written as:

$$\mathbf{T}(\mathcal{G}) = \mathbf{y} + \mathbf{r} \quad (2)$$

where $\mathbf{T}(\mathcal{G})$ implies the predicted temperature distribution data from equation (1); \mathcal{G} stands for unknown variables; \mathbf{y} means the temperature measurement data; \mathbf{r} represents the measurement noises. In light of the ill-posed attribute, the major challenge in solving the IHCP stems from the solution of the inverse problem. In accordance with the optimization theory and the Tikhonov regularization method, the solution of equation (2) is often cast into an optimization problem.

2.3. Generalized inversion model

In equation (2), the inaccurate property of the measurement data is highlighted. In practical applications, however, the computation of the forward problems may be inaccurate derived from the facts such as (1) the assumptions and simplifications of a real physical problem; (2) the imprecise initial conditions, boundary conditions, geometric conditions and thermal physical properties of materials; and (3) the discretization of the original problems and the approximation of the numerical computation. In this study, an inversion model is put forward to emphasize the above inaccurate attributes, which can be formulated as:

$$\mathbf{T}(\mathcal{G}) + \mathbf{B} = \mathbf{y} + \mathbf{r} \quad (3)$$

where \mathbf{B} represents the inaccurate attributes of the forward problem. It is necessary to mention that in the field of the econometrics equation (3) is also called as the semi-parametric regression model.

3. Design of the cost function

In accordance with the Tikhonov regularization method, the solution of equation (6) can be formulated into the following optimization problem:

$$\min_{\mathcal{G}, \mathbf{B}} \{E(\mathcal{G}, \mathbf{B}) + \alpha_1 \Omega_1(\mathcal{G}) + \alpha_2 \Omega_2(\mathbf{B})\} \quad (4)$$

where $E(\mathcal{G}, \mathbf{B})$ measures the data fidelity; Ω_1 and Ω_2 mean the regularizers; α_1 and α_2 are the regularization parameters.

In this study, the combination estimation that integrates the superiorities of the least squares estimation and the M-estimation is used to measure the data fidelity [17], which is specified as:

$$\min_{\mathcal{G}, \mathbf{B}} \left\{ (1 - \delta) \|T(\mathcal{G}) + \mathbf{B} - \mathbf{y}\|^2 + \delta \sum_{j=1}^m \rho(T(\mathcal{G})_j + \mathbf{B}_j - \mathbf{y}_j) + \alpha_1 \Omega_1(\mathcal{G}) + \alpha_2 \Omega_2(\mathbf{B}) \right\} \quad (5)$$

where $0 \leq \delta \leq 1$; $\|\cdot\|$ defines the 2-norm and $\rho(\cdot)$ means an M-estimation function [17-19]. In this study, the regularizers are defined as:

$$\Omega_1(\mathcal{G}) = \sum_{j=1}^m |\mathcal{G}_j|^p \quad (6)$$

$$\Omega_2(\mathbf{B}) = \|\mathbf{B}\|^2 \quad (7)$$

where $p > 0$, and $|\cdot|$ is an absolute value operator.

For convenient computations, the absolute value function is approximated by [20]:

$$|x| \approx (x^2 + \varepsilon)^{1/2} \quad (8)$$

where $\varepsilon > 0$ is a predetermined parameter. As a result, equation (9) can be approximated by:

$$\Omega_1(\mathcal{G}) \approx \sum_{j=1}^m (\mathcal{G}_j^2 + \varepsilon)^{p/2} \quad (9)$$

In this work, the G-M function is employed, which can be formulated by:

$$f(x) = 0.5x^2 / (\beta + x^2) \quad (10)$$

where $\beta > 0$ is a scaling parameter.

Finally, we can obtain a generalized cost function for solving the IHCP, i.e.

$$\min_{\mathbf{g}, \mathbf{B}} \left\{ (1-\delta) \|\mathbf{r}\|^2 + \delta \sum_{j=1}^m \frac{1}{2} \frac{\mathbf{r}_j^2}{\beta + \mathbf{r}_j^2} + \alpha_1 \sum_{j=1}^m (\mathbf{g}_j^2 + \varepsilon)^{p/2} + \alpha_2 \|\mathbf{B}\|^2 \right\} \quad (11)$$

where $\mathbf{r}_j = T(\mathbf{g})_j + \mathbf{B}_j - \mathbf{y}_j$.

4. Solving of the cost function

The direct solution of equation (11) is challenging. In accordance with the computational strategy reported in [21-23], equation (11) can be decoupled as the following sub-problems:

$$\mathbf{g}^{k+1} = \min_{\mathbf{g}} \left\{ (1-\delta) \|\mathbf{r}\|^2 + \delta \sum_{j=1}^m \frac{1}{2} \frac{\mathbf{r}_j^2}{\beta + \mathbf{r}_j^2} + \alpha_1 \sum_{j=1}^m (\mathbf{g}_j^2 + \varepsilon)^{p/2} \right\} \quad (12)$$

$$\mathbf{B}^{k+1} = \min_{\mathbf{B}} \left\{ (1-\delta) \|\mathbf{r}\|^2 + \delta \sum_{j=1}^m \frac{1}{2} \frac{\mathbf{r}_j^2}{\beta + \mathbf{r}_j^2} + \alpha_2 \|\mathbf{B}\|^2 \right\} \quad (13)$$

where superscript k represents the index of iterations.

Due to the excellent numerical performances, the BFGS algorithm is used to minimize equations (12) and (13), and the computation flowchart can be outlined as follows [24, 25]:

Step 1. Determine the cost function $\psi(\mathbf{x})$, and specify the initial value $\mathbf{x}^{(0)}$ and other algorithmic parameters.

Step 2. Set $\mathbf{H}_0 = \mathbf{I}_n$, estimate the gradient $\mathbf{g}_0 = \nabla \psi(\mathbf{x}^{(0)})$, and let $k \leftarrow 0$.

Step 3. Update the search direction:

$$\mathbf{d}^{(k)} = -\mathbf{H}_k \mathbf{g}_k \quad (14)$$

Step 4. Set

$$\mathbf{x}^{(k+1)} = \mathbf{x}^{(k)} + \alpha_k \mathbf{d}^{(k)} \quad (15)$$

$$\mathbf{g}_{k+1} = \nabla \psi(\mathbf{x}^{(k+1)}) \quad (16)$$

where α_k can be computed by solving the following minimization problem:

$$\psi(\mathbf{x}^{(k)} + \alpha_k \mathbf{d}^{(k)}) = \min_{\gamma \geq 0} \psi(\mathbf{x}^{(k)} + \gamma \mathbf{d}^{(k)}) \quad (17)$$

Step 5. If $\|\mathbf{g}_{k+1}\| \leq \varepsilon$, terminate the iteration and output the solution; otherwise return to Step 6.

Step 6. Set $\mathbf{u}^{(k)} = \mathbf{x}^{(k+1)} - \mathbf{x}^{(k)}$, $\boldsymbol{\ell}^{(k)} = \mathbf{g}_{k+1} - \mathbf{g}_k$, and compute \mathbf{H}_{k+1} using equation (18); set $k \leftarrow k+1$, and loop to Step 3.

$$\mathbf{H}_{k+1} = \mathbf{H}_k + \left(1 + \frac{\boldsymbol{\ell}^{(k)T} \mathbf{H}_k \boldsymbol{\ell}^{(k)}}{\mathbf{u}^{(k)T} \boldsymbol{\ell}^{(k)}} \right) \frac{\mathbf{u}^{(k)} \mathbf{u}^{(k)T}}{\mathbf{u}^{(k)T} \boldsymbol{\ell}^{(k)}} - \frac{\mathbf{u}^{(k)} \boldsymbol{\ell}^{(k)T} \mathbf{H}_k + \mathbf{H}_k \boldsymbol{\ell}^{(k)} \mathbf{u}^{(k)T}}{\mathbf{u}^{(k)T} \boldsymbol{\ell}^{(k)}} \quad (18)$$

Eventually, we obtain the following iterative technique to solve equation (11):

Step 1. Specify the algorithmic parameters and initial solutions of the unknown variables \mathcal{G} and \mathcal{B} .

Step 2. Update variable \mathcal{G} via solving equation (12) using the BFGS algorithm.

Step 3. Update variable \mathcal{B} via solving equation (13) using the BFGS algorithm.

Step 4. Return to Step 2 until a predetermined stopping condition is met.

5. Numerical experiments and discussions

The proposed inversion procedure is called as the generalized semiparametric inversion (GSI) algorithm. In this section, numerical experiments are implemented to test the performances of the GSI algorithm, and the inversion quality is compared with the STR method.

All algorithms are implemented using the MATLAB software. The forward problems are calculated by the finite element method. We use the relative errors (RE) to assess the inversion quality, which can be specified as follows:

$$\text{RE} = \frac{\|\mathcal{G}_{\text{True}} - \mathcal{G}_{\text{Estimated}}\|}{\|\mathcal{G}_{\text{True}}\|} \times 100\% \quad (19)$$

where $\mathcal{G}_{\text{True}}$ and $\mathcal{G}_{\text{Estimated}}$ mean the true values and the estimated values, respectively.

5.1. Case 1

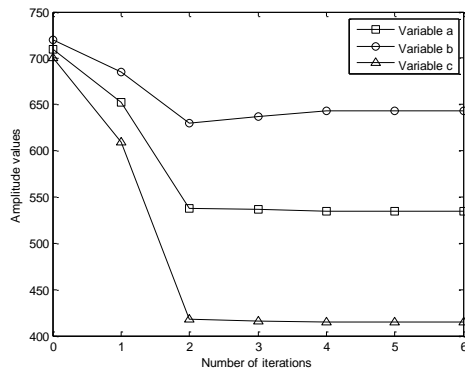
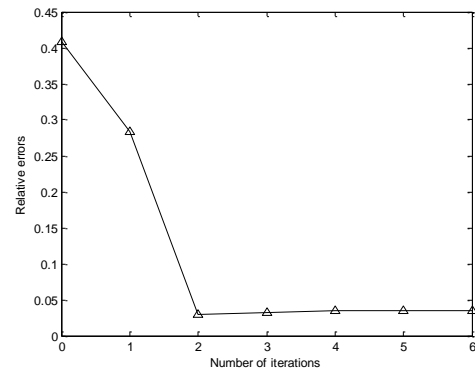
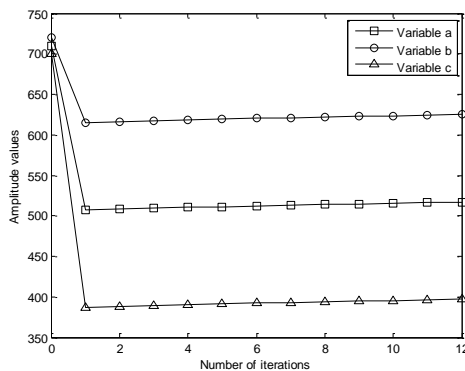
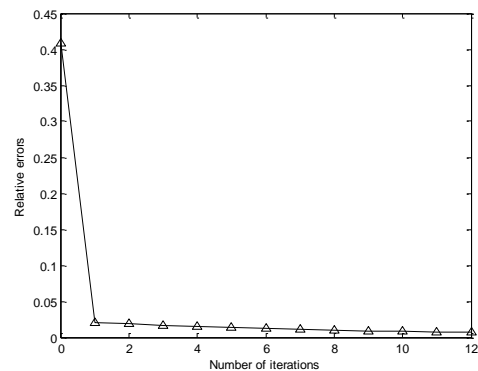
An inversion task of the three boundary conditions is implemented to test the efficiency of the GSI algorithm, and the forward problem is described by:

$$\rho c_p \frac{\partial T}{\partial t} = \lambda \left(\frac{\partial^2 T}{\partial x^2} + \frac{\partial^2 T}{\partial y^2} \right) \quad (20)$$

$$\begin{cases} T(x, y, t) = 520, & x = 0, 0 \leq y \leq 0.6 \\ T(x, y, t) = 620, & y = 0.6, 0 \leq x \leq 0.8 \\ T(x, y, t) = 400, & x = 0.8, 0 \leq y \leq 0.6 \\ -\lambda \partial T / \partial y = \varphi(x), & y = 0, 0 \leq x \leq 0.8 \\ T(x, y, 0) = 300 & 0 \leq x \leq 0.8, 0 \leq y \leq 0.6 \\ T(x, y, t) = 400, & (x - 0.4)^2 + (y - 0.3)^2 = 0.1^2 \end{cases} \quad (21)$$

where $\varphi(x) = 8000 + 3000 \sin(2.5x\pi / 0.8)$, $\rho = 8700 \text{ kg/m}^3$, $t \in [0, 300]$, $c_p = 385 \text{ J/(kg} \cdot \text{K)}$ and $\lambda = 400 \text{ W/(m} \cdot \text{K)}$.

The inverse problem estimates the boundary conditions, a , b and c , at $x = 0$, $y = 0.6$ and $x = 0.8$ from the given temperature data, and the true values for a , b and c are 520, 620 and 400. The simulated data is used to serve as the temperature measurement data. To simulate the inaccuracy of the forward problem, boundary condition at $(x - 0.4)^2 + (y - 0.3)^2 = 0.1^2$ is perturbed into 780. The algorithmic parameters of the GSI algorithm are defined as $\delta = 0$, $\alpha_1 = 0.0001$, $\alpha_2 = 0.04$ and $p = 1$. The regularization parameter for the STR method is 3×10^{-6} . The initial values of variables a , b and c for the both methods are 710, 720 and 700, respectively. Figures 1-4 are the estimation results and the REs for the competitors.

**Figure 1.** Estimated results for the STR method.**Figure 2.** Relative errors for the STR method.**Figure 3.** Estimated results for the GSI algorithm.**Figure 4.** Relative errors for the GSI algorithm.

The estimation results and the relative errors from the STR technique are illustrated in Figures 1 and 2. Numerical simulation results indicate that the STR method can ensure a stable inversion solution. Nevertheless, the final inversion results are not satisfactory. Especially, the final estimation results for a , b and c are 537.44, 629.41 and 417.94, and the RE, 2.96%, is higher than the GSI technique. Besides, in Figure 2, it can be found that the inaccuracy of the forward problem results in the oscillation of the solutions in the process of the numerical computation.

The result estimated by the GSI algorithm is shown in Figure 3. Numerical simulation results confirm that the GSI algorithm can alleviate the numerical instability of the IHCP in light of the fact that the Tikhonov regularization method is introduced to the cost function. With the consideration of the inaccuracy of the forward problem, the GSI algorithm shows satisfactory numerical performances, and the estimation results of variables a , b and c gradually approximate the true values with the increment of the number of iterations. In Figure 3, the final inversion results for variables a , b and c are 517.01, 625.14 and 397.70, which closely approximates the true values, 520, 620 and 400. In Figure 4, the REs monotonously decrease with the increase of the number of iterations, and the final RE of the GSI method is 0.74%, which is far lower than that of the STR technique. The encouraging results indicate that the GSI algorithm is competent in solving the IHCP.

5.2. Case 2

In this case, a complex inversion problem of the time-varying nonlinear boundary condition is simulated. The boundary condition at $y = 0$ is $\varphi(t) = a + b\sin(\pi t / 150)$, in which $a = 500$ and $b = 400$. The forward problem is described by:

$$\rho c_p \frac{\partial T}{\partial t} = \lambda \left(\frac{\partial^2 T}{\partial x^2} + \frac{\partial^2 T}{\partial y^2} \right) \tag{22}$$

$$\begin{cases} T(x, y, t) = 400, & x = 0, 0 \leq y \leq 0.6 \\ T(x, y, t) = 450, & y = 0.6, 0 \leq x \leq 0.8 \\ T(x, y, t) = 700, & x = 0.8, 0 \leq y \leq 0.6 \\ T(x, y, t) = \varphi(t), & y = 0, 0 \leq x \leq 0.8 \\ T(x, y, 0) = 300 & 0 \leq x \leq 0.8, 0 \leq y \leq 0.6 \\ T(x, y, t) = 800, & (x - 0.4)^2 + (y - 0.3)^2 = 0.1^2 \end{cases} \tag{23}$$

where $\lambda = 400 \text{ W}/(\text{m} \cdot \text{K})$, $\rho = 8700 \text{ kg}/\text{m}^3$, $t \in [0, 150]$ and $c_p = 385 \text{ J}/(\text{kg} \cdot \text{K})$.

The inverse problem estimates the boundary condition at $y = 0$. For easy calculation, the variables a and b in the formula of the boundary condition are estimated. Boundary conditions at $x = 0$, $y = 0.6$, $x = 0.8$ and $(x - 0.4)^2 + (y - 0.3)^2 = 0.1^2$ are perturbed into 380, 480, 690 and 780 to simulate the inaccuracies of the forward problem. The regularization parameter of the STR method is defined as 1×10^{-5} . The algorithmic parameters of the GSI algorithm are specified as $\delta = 0$, $\alpha_1 = 0.01$ and $\alpha_2 = 1 \times 10^{-4}$. The initial values for the both algorithms are 660 and 300. The estimation results and the REs for the STR technique and the GSI algorithm are shown in Figures 5-8. The REs for the both methods are presented in Figure 9.

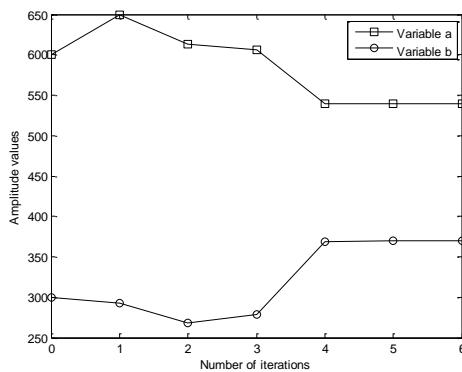


Figure 5. Estimated results by the STR method.

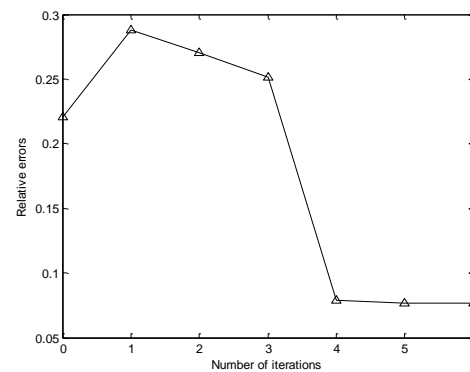


Figure 6. Relative errors for the STR method.

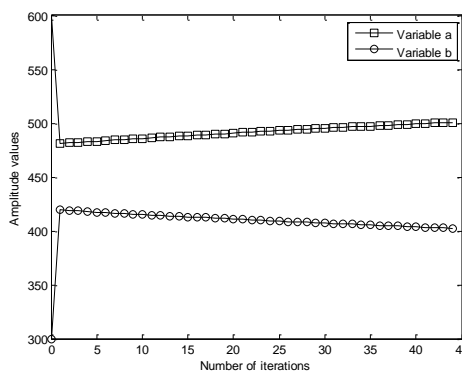


Figure 7. Estimated results by the GSI algorithm.

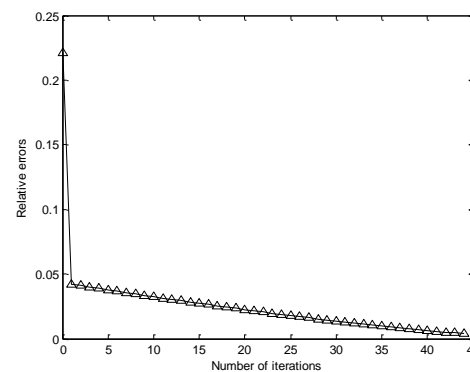


Figure 8. Relative errors for the GSI algorithm.

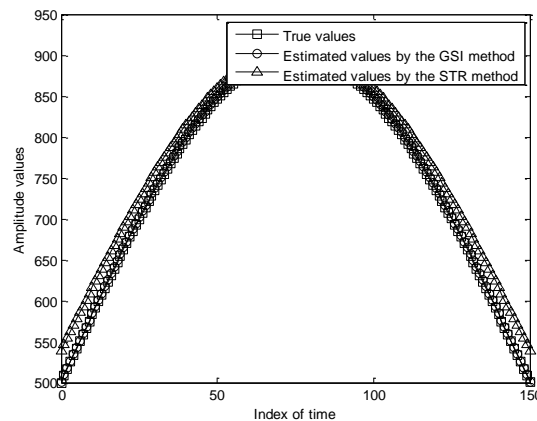


Figure 9. Final estimation results of the GSI method and the STR algorithm.

The estimation results and the REs for the STR method are presented in Figures 5 and 6, respectively. For the STR method, the final estimation results for unknown variables a and b are 539.24 and 370.42, and the RE is 7.67%. Obviously, the estimation accuracy of the STR method is lower than that of the GSI method.

The estimation results of the GSI technique for variables a and b are presented in Figure 7. As can be expected, for the time-varying inversion problem, the GSI algorithm shows satisfactory numerical performances. The final estimation results for variables a and b are 500.83 and 402.50, which approximates the true values, 500 and 400. Meanwhile, it can be seen from Figure 8 that the REs gradually decreases with the increase of the number of iterations, and the final RE is 0.41%, which is far lower than the STR technique.

Figure 9 presents the final boundary condition estimation results for the both methods. Obviously, when the inaccuracy of the forward problem is emphasized, the final estimation results from the GSI algorithm are in a better agreement with true boundary conditions as compared with the STR method, which indicate that the GSI method is highly suitable for solving the IHCP.

6. Conclusion

Different from traditional inversion methods, in this study a new inversion model that simultaneously highlights the measurement errors and the inaccurate properties of the forward problem is proposed to improve the inversion accuracy and robustness. With the assistance of the Tikhonov regularization method, a cost function is constructed to convert the original IHCP into an optimization problem. An iterative scheme that splits a complicated optimization problem into several simpler sub-problems and integrates the superiorities of the alternative optimization technique and the BFGS algorithm is developed to search for the optimal solution of the proposed cost function. Numerical experiment results indicate that the proposed method can ensure a stable numerical solution and improve the inversion accuracy and robustness, and the numerical implementation is easy. For the cases simulated in this study, excellent numerical performances and satisfactory results are observed, which indicates that the proposed algorithm is competent in solving the IHCP. As a consequence, a promising inversion algorithm is introduced for the solution of the IHCP.

References

- [1] K.W. Kim, S.W. Baek, Inverse radiation-conduction design problem in a participating concentric cylindrical medium, *International Journal of Heat and Mass Transfer*. 50 (2007) 2828-2837.
- [2] S.K. Singh, M.K. Yadav, R. Sonawane, S. Khandekar, K. Muralidhar, Estimation of time-dependent wall heat flux from single thermocouple data, *International Journal of Thermal*

- Sciences. 115 (2017) 1-15.
- [3] T. Liu, B. Liu, P.X. Jiang, Y.W. Zhang, H. Li, A two-dimensional inverse heat conduction problem in estimating the fluid temperature in a pipeline, *Applied Thermal Engineering*. 30 (2010) 1574-1579.
- [4] C.H. Huang, S.P. Wang, A three-dimensional inverse heat conduction problem in estimating surface heat flux by conjugate gradient method, *International Journal of Heat and Mass Transfer*. 42 (1999) 3387-3403.
- [5] A.N. Tikhonov, V.Y. Arsenin, *Solution of Ill-posed Problems*, V.H. Winston & Sons, Washington, 1977.
- [6] F.B. Liu, Particle swarm optimization-based algorithms for solving inverse heat conduction problems of estimating surface heat flux, *International Journal of Heat and Mass Transfer*. 55 (2012) 2062-2068.
- [7] K.H. Lee, S.W. Baek, K.W. Kim, Inverse radiation analysis using repulsive particle swarm optimization, *International Journal of Heat and Mass Transfer*. 51 (2008) 2772-2783.
- [8] B. Czél, G. Gróf, Inverse identification of temperature-dependent thermal conductivity via genetic algorithm with cost function-based rearrangement of genes, *International Journal of Heat and Mass Transfer*. 55 (2012) 4254-4263.
- [9] C.S. Liu, A self-adaptive LGSM to recover initial condition or heat source of one-dimensional heat conduction equation by using only minimal boundary thermal data, *International Journal of Heat and Mass Transfer*. 54 (2011) 1305-1312.
- [10] J.A.M. García, J.M.G. Cabeza, A.C. Rodríguez, Two-dimensional non-linear inverse problem heat conduction problem based on the singular value decomposition, *International Journal of Thermal Sciences*. 48 (2009) 1081-1093.
- [11] F.B. Liu, A modified genetic algorithm for solving the inverse heat transfer problem of estimating plan heat source, *International Journal of Heat and Mass Transfer*. 51 (2008) 3745-3752.
- [12] S. Deng, Y. Hwang, Applying neural networks to the solution of forward and the inverse heat conduction problems, *International Journal of Heat and Mass Transfer*. 49 (2006) 4732-4750.
- [13] M.N. Ozisik, H.R.B. Orlande, *Inverse Heat Transfer*, Taylor & Francis, New York, 2000.
- [14] O.M. Alifanov, *Inverse Heat Transfer Problems*, Springer-Verlag, New York, 1994.
- [15] J.V. Beck, B. Blackwell, C.R. Clair, *Inverse Heat Conduction: Ill-posed Problems*, Wiley, New York, 1985.
- [16] R.T. Lin, *Theory and Methods on the Heat Conduction*, Tianjin University Press, Tianjin, 1992.
- [17] Y. Dodge, J. Jureckova, *Adaptive Regression*, Springer-Verlag, New York, 2000.
- [18] P.J. Huber, *Robust Statistics*, John Wiley & Sons, New York, 1981.
- [19] T. Wang, *Methods on robust estimation and detection of multiple outliers in linear regression*, Ph.D. Dissertation, The Fourth Military Medical University, 2000.
- [20] R. Acar, C.R. Vogel, Analysis of bounded variation penalty methods for ill posed problem, *Inverse Problems*. 10 (1994) 1217-1229.
- [21] J. Lei, W.Y. Liu, Q.B. Liu, X.Y. Wang, S. Liu, Shearlet regularization and dimensionality reduction for the temperature distribution sensing, *Measurement*, 82 (2016) 176-187.
- [22] Y. Xiao, T. Zeng, J. Yu, M.K. Ng, Restoration of images corrupted by mixed Gaussian-impulse noise via L1-L0 minimization, *Pattern Recognition*. 44 (2011) 1708-1720.
- [23] X.G. Lv, Y.Z. Song, S.X. Wang, J. Le, Image restoration with a high-order total variation minimization method, *Applied Mathematical Modelling*. 37 (2013) 8210-8224.
- [24] J. Nocedal, S.J. Wright, *Numerical Optimization*, Science Press, Beijing, 2006.
- [25] Z.H. Ma, *Handbook of Modern Applied Mathematics: Operation Research and Optimization Theory*, Tsinghua University Press, Beijing, 1998.